

A Fast 3D Poisson Solver of Arbitrary Order Accuracy

E. Braverman,* M. Israeli,* A. Averbuch,† and L. Vozovoi†

**Technion-Israel Institute of Technology, Computer Science Department, Haifa 32000, Israel;*

and †School of Mathematical Sciences, Tel Aviv University, Tel Aviv 69978, Israel

E-mail: maelena@cs.technion.ac.il, israeli@cs.technion.ac.il,

amir@math.tau.ac.il, and vozovoi@math.tau.ac.il

Received August 19, 1997; revised April 20, 1998

We present a direct solver for the Poisson and Laplace equations in a 3D rectangular box. The method is based on the application of the discrete Fourier transform accompanied by a subtraction technique which allows reducing the errors associated with the Gibbs phenomenon and achieving any prescribed rate of convergence. The algorithm requires $O(N^3 \log N)$ operations, where N is the number of grid points in each direction. We show that our approach allows accurate treatment of singular cases which arise when the boundary function is discontinuous or incompatible with the differential equation. © 1998 Academic Press

Key Words: 3D Poisson solver for Dirichlet problem; Fourier method; corner and edge singularities.

1. INTRODUCTION

Fast and accurate solution of elliptic equations is an important step towards resolution of problems which appear in computational physics or fluid dynamics (CFD). These equations arise in the determination of the pressure field for incompressible CFD, in the implicit solution of viscous and heat transfer problems, in the solution of the Maxwell equations for lithographic exposure, in the solution of reaction-diffusion equations for baking and dissolution processes in semiconductor manufacture and in many other applications.

We solve the Poisson equation in a 3D domain. Most Poisson and Laplace solvers were initially developed for the 2D case, such as the iterative multigrid techniques [15], domain decomposition [9] and other preconditioning strategies, the boundary integral method [16], and the adaptive [11] fast multipole method [12].

Application of high-order (pseudo) spectral methods, which are based on global expansions into orthogonal polynomials (Chebyshev or Legendre polynomials), to the solution of elliptic equations, results in full matrix problems. The cost of inverting full $P \times P$ matrices

without using special properties is $O(P^3)$ operations [8]. Besides, the accuracy may decrease considerably as the dimension N^2 of the system grows due to accumulation of round-off errors. These remarks are related to the 2D case, where in 3D the cost increases drastically. Sparse representations which can be derived by the application of the wavelet transform to elliptic operators can reduce the number of operations as it is described in [2, 3].

The Fourier method has the following advantages when it is used to solve the Laplace (Poisson) equation:

1. Differential operators are represented in the Fourier basis by diagonal matrices which reduce the integration to division of the Fourier coefficients by the corresponding wave numbers.
2. If the function is infinitely differentiable and periodic then the approximation of f by Fourier series converges to f more rapidly than any finite power of $1/N$, where N is the number of Fourier harmonics.

Multidimensional FFT can be immediately applied to a regular domain (rectangle in 2D and parallelepiped in 3D). Besides, rapid convergence assumes periodicity of the function and its derivatives up to a certain order. If the function is nonperiodic, the Fourier series converges as $1/N$, where N is the number of points in each direction, which is not better than a first-order finite-difference scheme. In [4, 5] a fast 2D algorithm was developed which incorporates the application of the FFT with a preliminary subtraction technique. The method requires $O(N^2 \log N)$ operations for N^2 discretization points in the 2D case and can achieve any prescribed rate of convergence. In this paper we generalize the algorithm to a 3D case. The efficiency of the algorithm is especially vital for 3D problems which usually require heavy computations. The method which is presented here enjoys the properties of the 2D algorithm: fast convergence (i.e., small N necessary to achieve the prescribed accuracy) and comparatively small number of operations per point ($O(\log N)$).

We consider the Poisson equation

$$\Delta u = f \tag{1.1}$$

with Dirichlet boundary conditions.

First, a particular solution of (1.1) is obtained; then an auxiliary problem for the Laplace equation is solved. The boundary conditions for the auxiliary problem are obtained as the difference between the original boundary conditions and those obtained from the particular solution. If the particular solution corresponds to zero boundary values, then we solve the Laplace equation with the original boundary conditions.

Thus, the algorithm consists of two steps:

- Step 1.* solving a Poisson equation (1.1) with some boundary conditions;
- Step 2.* solving a Laplace equation with specified boundary conditions.

Below we describe two steps of the algorithm and characterize the methods which are used to avoid the Gibbs phenomenon.

1. The function f in the right-hand side of Eq. (1.1) is extended to a larger domain and it is replaced by a new function which coincides with f in the original domain and it is periodic together with a certain number of its derivatives in the larger domain [4, 18]. This procedure is based on the local Fourier basis method [14, 19] and it uses the folding operation as it is described in [1, 13].

2. The auxiliary boundary value problem for the Laplace equation is solved to satisfy the original boundary conditions. Here we restrict ourselves to a Dirichlet problem. We reduce the effect of the Gibbs phenomenon by employing the subtraction technique used in [5], which is extended to the 3D case. The boundary conditions are represented as a sum of periodic functions with functions which are considered as a restriction of the known harmonic functions to the boundaries. In particular, combinations of the functions

$$f_1(x, y, z) = \sin \lambda_1 x \sin \lambda_2 y \sinh \lambda_3 z, \quad \lambda_1^2 + \lambda_2^2 = \lambda_3^2, \quad (1.2)$$

$$f_2(x, y, z) = \sin \lambda_1 x \sinh \lambda_2 y \sinh \lambda_3 z, \quad \lambda_1^2 = \lambda_2^2 + \lambda_3^2, \quad (1.3)$$

enjoy the property $f_i(1, 1, 1) \neq 0$ and $f_i(x, y, z) = 0$ in all the other corners. By subtracting one of the weighted functions (1.2) or (1.3) we achieve the zero value in the corner (1, 1, 1) without affecting the values on the other corners. Eight functions are subtracted to achieve zero values on the corners; then the second derivatives in the corners are eliminated, etc. A similar procedure is applied to the edges. Finally, the solution is derived by the application of the discrete sine transform (DST) to each of the six faces, where the boundary conditions are eventually periodic.

The present paper employs the following ideas of [4, 5]. First, the Gibbs phenomena is reduced by subtraction of some harmonic functions. Second, these subtraction functions are chosen as products of trigonometric (i.e., cos, sin, cosh, sinh) functions. However, for the 3D case the algorithm is more complicated because in 2D the subtraction step was concerned only with the corners, while in the 3D case we have to treat both corners and edges. Therefore, different subtraction functions have to be derived. In addition, in [17] and [5] singular cases were treated when the boundary function is discontinuous or nonharmonic on the corner of the 2D rectangular. The spectral accuracy was restored by subtracting the singularity. The singularity treatment of the 3D case is much more difficult by the following reasons. First, we may have discontinuity not only at one point but along the whole edge. Second, we cannot use the methods from complex analysis which were useful in removing the 2D singularities. Therefore, the whole mechanism to remove singularities in the 3D case is new.

The method which is presented here can be modified and extended to handle Neumann/mixed boundary conditions and for an elliptic equation of a more general type as in [6].

The paper has the following structure. In Section 2 we solve the boundary value problem for the Laplace equation. We describe the procedure that leads to the boundary function which vanishes on the corners. The same technique is applied to eliminate the derivatives. Section 2.3 describes the algorithm which transforms the boundary function to a periodic one (together with its derivatives up to the third one) to avoid the Gibbs phenomenon. The outline of the algorithm with operations count and convergence rate estimates are given in the next section. Numerical results are presented in Section 2.6. Finally, certain singular cases are considered when the boundary function is discontinuous or does not satisfy the Laplace equation on a certain edge. Section 3 describes the application of the Fourier method for the solution of (1.1) in the 3D case.

2. LAPLACE EQUATION IN A BOX

2.1. Mathematical Preliminaries

Consider the Laplace equation in a cube. Let \mathcal{C} stand for the open cube $(0, \pi) \times (0, \pi) \times (0, \pi) = \{(x, y, z) : 0 \leq x < \pi, 0 < y < \pi, 0 < z < \pi\}$ and let $\partial\mathcal{C}$ stand for the boundary

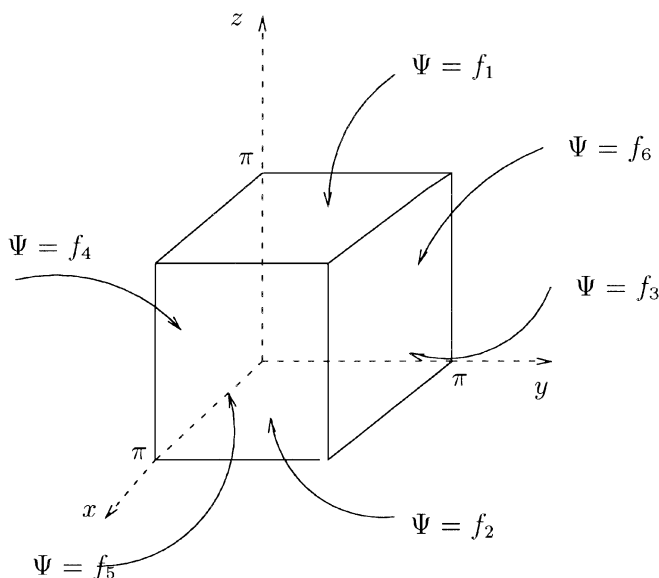


FIG. 1. Dirichlet problem for the cube C . The continuous function f on ∂C is specified by six functions f_1, \dots, f_6 , one on each of the six faces of ∂C .

surface of that cube. To solve the Dirichlet problem for \mathcal{C} (Fig. 1), we solve first a simpler problem:

$$\begin{aligned} \Delta \Psi &= \Psi_{xx} + \Psi_{yy} + \Psi_{zz} = 0 \\ \Psi(0+, y, z) &= \Psi(\pi-, y, z) = 0, \quad \Psi(x, 0+, z) = \Psi(x, \pi-, z) = 0 \\ \Psi(x, y, 0+) &= 0, \quad \Psi(x, y, \pi-) = f_1(x, y). \end{aligned} \quad (2.1)$$

Substituting $\Psi(x, y, z) = X(x)Y(y)Z(z)$ into Laplace's equation we obtain, upon dividing by $X(x)Y(y)Z(z)$,

$$\frac{X''(x)}{X(x)} + \frac{Y''(y)}{Y(y)} + \frac{Z''(z)}{Z(z)} = 0$$

and the homogeneous (zero) conditions in (2.1) yield

$$X(0) = X(\pi) = 0, \quad Y(0) = Y(\pi) = 0, \quad Z(0) = 0.$$

These last two results lead us to

$$\begin{aligned} X''(x) &= \lambda X(x), \quad Y''(y) = \mu Y(y), \quad Z''(z) = -(\lambda + \mu)Z(z) \\ X(0) &= X(\pi) = 0, \quad Y(0) = Y(\pi) = 0, \quad Z(0) = 0, \end{aligned} \quad (2.2)$$

where λ and μ are constants. The first two problems in (2.2) yield the same eigenvalues and eigenfunctions as the wave equation (for $a = b = \pi$). Substituting those eigenvalues $\lambda_m = -m^2$ and $\mu_n = -n^2$ into the third problem in (2.2), we find the solution

$$Z_{mn}(z) = \sinh \delta_{mn} z,$$

where $\delta_{mn} = (m^2 + n^2)^{1/2}$. Any finite superposition of these separable solutions,

$$\sum_{m,n=1}^{M,N} D_{mn} \sin mx \sin ny (\sinh \delta_{mn} z / \sinh \delta_{mn} \pi), \quad (2.3)$$

is harmonic. If $M, N \rightarrow \infty$ we obtain

$$\Psi(x, y, z) = \sum_{m,n=1}^{\infty} D_{mn} \sin mx \sin ny (\sinh \delta_{mn} z / \sinh \delta_{mn} \pi),$$

where the coefficients D_{mn} are yet to be determined. For $z = \pi$ to satisfy $\Psi = f_1$ it is required that

$$f_1 \sim \sum_{m,n=1}^{\infty} D_{mn} \sin mx \sin ny.$$

Therefore, the solution to (2.1) can be written as

$$\Psi(x, y, z) = \sum_{m,n=1}^{\infty} D_{mn} \sin mx \sin ny (\sinh \delta_{mn} z / \sinh \delta_{mn} \pi), \quad (2.4)$$

where $\delta_{mn} = (m^2 + n^2)^{1/2}$ is a solution of (2.1) (the detailed discussion is given in Appendix 1) and

$$D_{mn} = \frac{4}{\pi^2} \int_0^{\pi} \int_0^{\pi} f_1(x, y) \sin mx \sin ny \, dx \, dy. \quad (2.5)$$

By adding such solutions we obtain the solution Ψ to the general Dirichlet problem as a sum of six series like the one of (2.4). Similarly, the problem

$$\Delta \Psi = 0$$

$$\Psi(0+, y, z) = \Psi(\pi-, y, z) = 0$$

$$\Psi(x, 0+, z) = f_4(x, z), \quad \Psi(x, \pi-, z) = 0$$

$$\Psi(x, y, 0+) = \Psi(x, y, \pi-) = 0$$

has the series solution

$$\Psi(x, y, z) = \sum_{m,n=1}^{\infty} D_{mn} \sin mx \sin nz \frac{\sinh \delta_{mn}(\pi - y)}{\sinh \delta_{mn} \pi},$$

where

$$D_{mn} = \frac{4}{\pi^2} \int_0^{\pi} \int_0^{\pi} f_4(u, v) \sin mu \sin nv \, du \, dv.$$

The other four series solution needed for the solution can be obtained by permuting the variables $x, y,$ and z in the two series above.

The validity of (2.4) as a solution to (2.1) is discussed in Appendix 1.

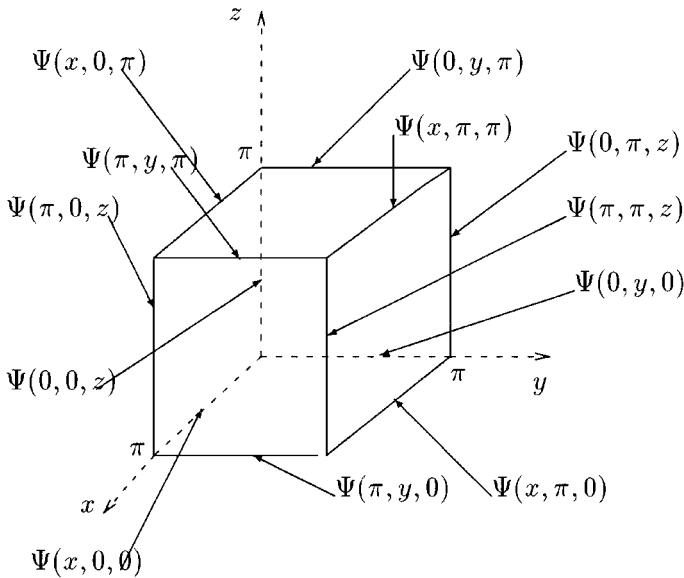


FIG. 2. Dirichlet's problem for cube C . Here the solution $\Psi(x, y, z)$ is specified on the twelve edges of C .

2.2. Subtraction Procedure for Edges

A sum of six series like the one in Eq. (2.4) is a solution of the Laplace equation with the given boundary function on the surface ∂C . However, if $\Psi \neq 0$ on the edges of the cube, the convergence of the series will be very slow because of the Gibbs phenomenon. Convergence can be improved if the face functions vanish together with their even derivatives to some order. For example, zeroing out the function Ψ on the edge $y = 0, z = \pi, 0 < x < \pi$, can be achieved by subtraction of the function (Fig. 2):

$$u_1(x, y, z) = \sum_{n=1}^{\infty} d_n \sin nx \frac{\sinh \lambda_{1n}(\pi - y)}{\sinh \lambda_{1n}\pi} \frac{\sinh \lambda_{2n}z}{\sinh \lambda_{2n}\pi}, \quad (2.6)$$

where $\lambda_{1n}^2 + \lambda_{2n}^2 = n^2$, or alternatively,

$$u_1^*(x, y, z) = \sum_{n=1}^{\infty} d_n \sin nx \frac{\sinh \lambda_{1n}(\pi - y)}{\sinh \lambda_{1n}\pi} \frac{\sin \lambda_{2n}z}{\sin \lambda_{2n}\pi} \quad (2.7)$$

with $\lambda_{1n}^2 - \lambda_{2n}^2 = n^2$, where we must require the "nonresonance condition" $\sin \lambda_{2n}\pi \neq 0$. Here

$$d_n = \frac{2}{\pi} \int_0^{\pi} \Psi(x, 0, \pi) \sin nx \, dx;$$

u_1 and u_1^* are obviously harmonic and vanish on all the edges except the one under consideration.

Similarly,

$$u_2(x, y, z) = \sum_{n=1}^{\infty} \left[\frac{2}{\pi} \int_0^{\pi} \Psi(x, 0, \pi) \sin nx \, dx \right] \sin nx \frac{\sinh \lambda_{1n}y}{\sinh \lambda_{1n}\pi} \frac{\sinh \lambda_{2n}z}{\sinh \lambda_{2n}\pi} \quad (2.8)$$

is appropriate for $\Psi(x, \pi, \pi) = 0, 0 < x < \pi,$

$$u_3(x, y, z) = \sum_{n=1}^{\infty} \left[\frac{2}{\pi} \int_0^{\pi} \Psi(x, 0, \pi) \sin nx \, dx \right] \sin nx \frac{\sinh \lambda_{1n}(\pi - y)}{\sinh \lambda_{1n}\pi} \frac{\sinh \lambda_{2n}(\pi - z)}{\sinh \lambda_{2n}\pi} \tag{2.9}$$

is appropriate for $\Psi(x, 0, 0) = 0, 0 < x < \pi,$ and

$$u_4(x, y, z) = \sum_{n=1}^{\infty} \left[\frac{2}{\pi} \int_0^{\pi} \Psi(x, 0, \pi) \sin nx \, dx \right] \sin nx \frac{\sinh \lambda_{1n}y}{\sinh \lambda_{1n}\pi} \frac{\sinh \lambda_{2n}(\pi - z)}{\sinh \lambda_{2n}\pi} \tag{2.10}$$

is appropriate for $\Psi(x, \pi, 0) = 0, 0 < x < \pi.$ The analogs of the functions (2.7) are obtained in a similar way.

Eight other subtraction functions can be obtained from (2.6)–(2.10) by permuting the variables $x, y,$ and $z.$

After subtracting u_1, u_2, \dots, u_{12} we will have a solution that vanishes on edges (except perhaps corners).

We observe that approximation of this solution by a series of type (2.4) will converge faster if the function vanishes on the edges, together with its even derivatives.

Let

$$\frac{\partial^2 \Psi}{\partial y^2}(x, 0, \pi) \sim \sum_{n=1}^{\infty} b_n \sin nx, \tag{2.11}$$

where

$$b_n = \frac{2}{\pi} \int_0^{\pi} \frac{\partial^2 \Psi}{\partial y^2}(x, 0, \pi) \sin nx \, dx. \tag{2.12}$$

The following function is subtracted for the elimination of the second derivative,

$$\sum_{n=1}^{\infty} \frac{b_n}{\lambda_{1n}^2 + \lambda_{2n}^2} \sin nx \left[\frac{\sinh \lambda_{1n}(\pi - y)}{\sinh \lambda_{1n}\pi} \frac{\sin \lambda_{2n}z}{\sin \lambda_{2n}\pi} - \frac{\sin \lambda_{2n}(\pi - y)}{\sin \lambda_{2n}\pi} \frac{\sinh \lambda_{1n}z}{\sinh \lambda_{1n}\pi} \right], \tag{2.13}$$

where b_n is defined in (2.12), $\lambda_{1n} > \lambda_{2n}, \sin \lambda_{1n} \neq 0, \sin \lambda_{2n} \neq 0,$ and $\lambda_{1n}^2 - \lambda_{2n}^2 = n^2.$ This function enjoys the following properties: it is harmonic, vanishes on all the edges together with its first derivatives, its second derivative in y vanishes on all the edges except the chosen one. It also has the same second derivative in z as the boundary conditions since here the boundary function is assumed to be harmonic.

Similarly, the annihilation of the fourth derivatives is achieved by subtracting a linear combination of the two functions (2.13) with different coefficients and frequencies.

Under certain conditions the subtraction of the edge values and the second derivatives can be achieved simultaneously as shown in Appendix 2.

We recall that a boundary function on the segment can be approximated by the sine series (4.4) if it vanishes on the ends. We proceed to describe the procedure for obtaining zeroes on the corners.

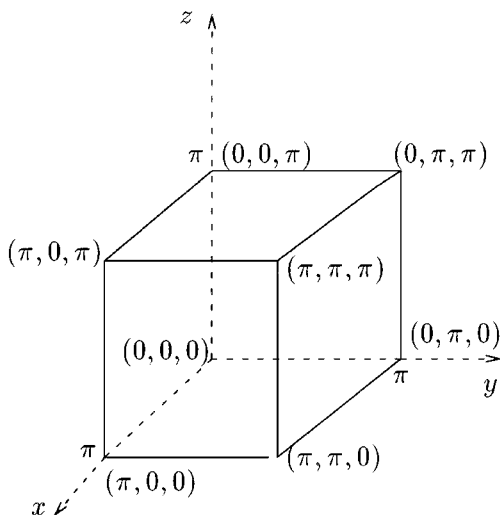


FIG. 3. Dirichlet's problem for cube C . Here the solution $\Psi(x, y, z)$ is specified on the eight corners of C .

2.3. Subtraction Procedure for Corners

Let $\Psi(0, 0, 0) = A$. A zero value at the origin is achieved by subtracting the so-called "corner functions" given by (Fig. 3):

$$C_{(0,0,0)}(x, y, z) = A \left[\frac{\sinh \lambda_1(\pi - x)}{\sinh \lambda_1 \pi} \frac{\sinh \lambda_2(\pi - y)}{\sinh \lambda_2 \pi} \frac{\sin \lambda_3(\pi - z)}{\sin \lambda_3 \pi} \right], \quad (2.14)$$

where the arguments can be changed to fit the other corners and $\lambda_1^2 + \lambda_2^2 = \lambda_3^2$. The subtraction of such a function does not influence the values in the seven other corners; thus each corner can be treated separately.

Denote

$$B_x = \frac{\partial^2 \Psi}{\partial x^2}(0, 0, 0), \quad B_y = \frac{\partial^2 \Psi}{\partial y^2}(0, 0, 0), \quad B_z = \frac{\partial^2 \Psi}{\partial z^2}(0, 0, 0).$$

The second derivative vanishes after subtracting a linear combination of the above functions. For example, in the case of $(B_y - B_x)(2B_x + B_y) > 0$ the function

$$a \left[\frac{\sinh \lambda_1(\pi - x)}{\sinh \lambda_1 \pi} \frac{\sinh \lambda_2(\pi - y)}{\sinh \lambda_2 \pi} \frac{\sin \lambda_3(\pi - z)}{\sin \lambda_3 \pi} - \frac{\sinh \lambda_2(\pi - x)}{\sinh \lambda_2 \pi} \frac{\sin \lambda_3(\pi - y)}{\sin \lambda_3 \pi} \frac{\sinh \lambda_1(\pi - z)}{\sinh \lambda_1 \pi} \right]$$

is subtracted, where $\operatorname{sgn}|a| = \operatorname{sgn}(B_y - B_x)$, and

$$\lambda_1^2 = \frac{2B_x + B_y}{3a}, \quad \lambda_2^2 = \frac{B_y - B_x}{3a}, \quad \lambda_3^2 = \lambda_1^2 + \lambda_2^2.$$

For $(B_y - B_x)(2B_x + B_y) < 0$ and $|2B_x + B_y| > |B_y - B_x|$ the subtraction function is chosen

as

$$a \left[\frac{\sinh \lambda_1(\pi - x)}{\sinh \lambda_1 \pi} \frac{\sin \lambda_2(\pi - y)}{\sin \lambda_2 \pi} \frac{\sin \lambda_3(\pi - z)}{\sin \lambda_3 \pi} - \frac{\sin \lambda_2(\pi - x)}{\sin \lambda_2 \pi} \frac{\sin \lambda_3(\pi - y)}{\sin \lambda_3 \pi} \frac{\sinh \lambda_1(\pi - z)}{\sinh \lambda_1 \pi} \right],$$

where a is of the same sign as $(B_x - B_y)$:

$$\lambda_1^2 = \frac{2B_x + B_y}{3a}, \quad \lambda_2^2 = \frac{B_x - B_y}{3a}, \quad \lambda_3^2 = \lambda_1^2 - \lambda_2^2.$$

For $(B_y - B_x)(2B_x + B_y) < 0$ and $|2B_x + B_y| < |B_y - B_x|$ we subtract

$$a \left[\frac{\sinh \lambda_1(\pi - x)}{\sinh \lambda_1 \pi} \frac{\sin \lambda_2(\pi - y)}{\sin \lambda_2 \pi} \frac{\sinh \lambda_3(\pi - z)}{\sinh \lambda_3 \pi} - \frac{\sin \lambda_2(\pi - x)}{\sin \lambda_2 \pi} \frac{\sinh \lambda_3(\pi - y)}{\sinh \lambda_3 \pi} \frac{\sinh \lambda_1(\pi - z)}{\sinh \lambda_1 \pi} \right]$$

with a, λ_1, λ_2 as in the previous case, $\lambda_3^2 = \lambda_2^2 - \lambda_1^2$.

In case $B_y = B_x$ we choose the subtraction function as

$$a \left[\frac{\sinh \lambda(\pi - x)}{\sinh \lambda \pi} \frac{\sinh \lambda(\pi - y)}{\sinh \lambda \pi} \frac{\sin \sqrt{2}\lambda(\pi - z)}{\sin \sqrt{2}\lambda \pi} - \frac{\sin \lambda(\pi - x)}{\sin \lambda \pi} \frac{\sin \lambda(\pi - y)}{\sin \lambda \pi} \frac{\sinh \sqrt{2}\lambda(\pi - z)}{\sinh \sqrt{2}\lambda \pi} \right],$$

where λ and a are such that $a\lambda^2 = B_x/2$.

For the case $B_y = -2B_x$ we subtract the same function as above, where y and z are permuted. The choice of λ and all λ_i should be such that the denominators do not vanish.

Similar functions are subtracted for the other corners. For instance, in the ‘‘corner function’’ of $(\pi, 0, \pi)$ in (2.14), (4.8), $\pi - x$ is changed by x and $\pi - z$ —by z etc.

If the boundary function does not vanish in the corner, the subtraction of the corner values and the second derivatives can be achieved simultaneously as shown in Appendix 2.

Figure 4 illustrates the values on the face $z = 0$ after subtraction of the corner functions and the edge functions, respectively, for the numerical solution of the Dirichlet problem in the cube $[0, 1] \times [0, 1] \times [0, 1]$ which corresponds to the exact solution

$$\Psi(x, y, z) = \frac{1}{\sqrt{(x - 0.5)^2 + (y - 0.5)^2 + (z - 0.5)^2}}.$$

The second derivatives were computed using the divided differences method which corresponds to a polynomial of the fourth order (four points in addition to one where the derivative is evaluated).

2.4. Steps of the Algorithm

1. Subtraction of corner functions defined by (2.14).

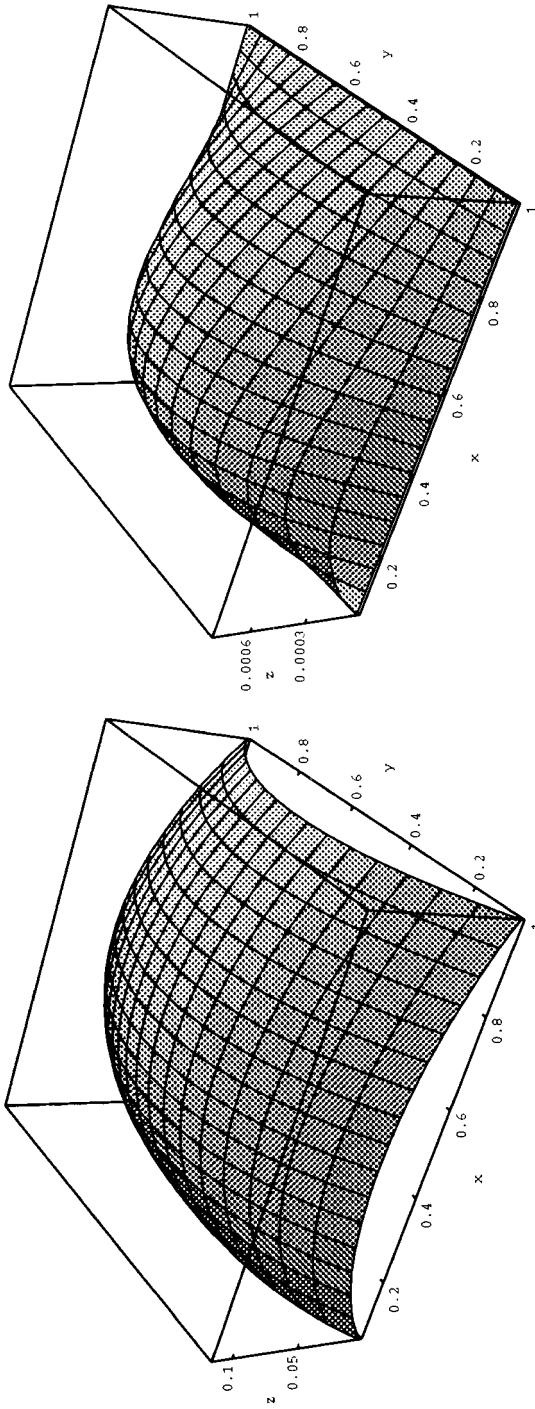


FIG. 4. The values on one of the faces after subtraction of corner functions and edge functions, respectively.

2. Computation of the second derivatives in two directions for each corner by the divided differences method.

3. Elimination of the second derivatives on the corners by using the subtracting functions which were defined in Section 2.3.

4. Application of the discrete sine transform (DST) on each of the 12 edges and subtraction of the “edge functions” (2.6) or (2.7).

5. Computation of the second derivatives in the orthogonal direction for the 12 edges.

6. Subtraction of 12 functions defined by (2.13).

7. Application of two-dimensional DST on the six faces; the remainder of the solution is in (2.3) form.

2.5. Rate of Convergence and Operation Count

The numerical error is dominated by the truncation of the Fourier series. We begin by estimating the accuracy of the two-dimensional approximation if we truncate the series in (2.4) for any of the six faces. Consider the first one. The tail of the truncated series,

$$\begin{aligned} & \left| \sum_{m,n=1}^{\infty} D_{mn} \sin mx \sin ny \frac{\sinh \delta_{mn} z}{\sinh \delta_{mn} \pi} - \sum_{m,n=1}^{M,N} D_{mn} \sin mx \sin ny \frac{\sinh \delta_{mn} z}{\sinh \delta_{mn} \pi} \right| \\ &= \left| \sum_{m=M+1}^{\infty} \sum_{n=1}^{\infty} D_{mn} \sin mx \sin ny + \sum_{m=1}^{\infty} \sum_{n=N+1}^{\infty} D_{mn} \sin mx \sin ny \right| \\ &\leq \sum_{m=M+1}^{\infty} \sum_{n=1}^{\infty} |D_{mn} \sin mx \sin ny| + \sum_{m=1}^{\infty} \sum_{n=N+1}^{\infty} |D_{mn} \sin mx \sin ny|, \end{aligned}$$

since $0 \leq \sinh \delta_{mn} z \leq \sinh \delta_{mn} \pi$ for $0 \leq z \leq \pi$.

Let f_1 be a periodic function with $k - 1$ periodic derivatives in x and $l - 1$ periodic derivatives in y , while $\partial^{k+l} f_1 / \partial x^k \partial y^l$ is integrable in $[0, \pi] \times [0, \pi]$. Applying integration by parts to (2.5) yields [10]

$$\begin{aligned} D_{mn} &= \frac{4}{\pi^2} \int_0^{\pi} \int_0^{\pi} f_1(x, y) \sin mx \sin ny \, dx \, dy \\ &= \frac{4}{\pi^2 m^k} \int_0^{\pi} \int_0^{\pi} \frac{\partial^k f_1(x, y)}{\partial x^k} \varphi_m(mx) \sin ny \, dx \, dy \\ &= \frac{4}{\pi^2 m^k} \int_0^{\pi} \int_0^{\pi} \frac{\partial^{k+l} f_1(x, y)}{\partial x^k \partial y^l} \varphi_m(mx) \varphi_l(ny) \, dx \, dy, \end{aligned}$$

where

$$\varphi_i(t) = \begin{cases} \cos t, & \text{odd } i, \\ \sin t, & \text{even } i. \end{cases}$$

Thus, $D_{mn} \ll 1/(m^k n^l)$ and the error estimate

$$\left| f_1(x, y) - \sum_{m,n=1}^{M,N} D_{mn} \sin mx \sin ny \right| = O\left(\frac{1}{n^l} + \frac{1}{m^k}\right) = O\left(\max\left\{\frac{1}{n^l}, \frac{1}{m^k}\right\}\right)$$

is valid for both the first face and the corresponding part of the solution in the cube. Therefore, if the function and its first derivative vanish on the boundaries (one subtraction step), then the maximal error is reduced by the factor of $2^2 = 4$ when the number of points is doubled in each direction. The maximal error is reduced by the factor of $2^4 = 16$ if all the derivatives up to the third one vanish on the boundaries (two step subtraction). Obviously, all the other steps of the algorithm (namely, one-dimensional sine Fourier transform for edges) have the same rate of convergence.

Operation Count

Let N be the number of grid points in each direction:

- | | |
|---|----------------------------|
| 1. Subtraction of corner functions (2.14) | $8 \cdot O(N^3)$ |
| 2. Computation of the second derivatives in two directions for each corner | $16 \cdot O(1)$ |
| 3. Elimination of the second derivatives in the corners | $8 \cdot O(N^3)$ |
| 4. Application of discrete sine transform for each of the 12 edges and subtraction of the "edge functions" (2.6) or (2.7) | $12 \cdot O(N^3 \log_2 N)$ |
| 5. Computation of the second derivatives in the orthogonal direction for the 12 edges | $12 \cdot O(N)$ |
| 6. The same procedure as in 4 for the second derivatives | $12 \cdot O(N^3 \log_2 N)$ |
| 7. Application of discrete sine transform for the six faces; construction and summation of the 6 solutions. | $6 \cdot O(N^3 \log_2 N)$ |

Therefore, the total computational cost of the algorithm is $32 \cdot O(N^3 \log_2 N) + O(N^3)$, i.e., $O(N^3 \log_2 N)$ operations.

2.6. Numerical Results

Assume that Ψ is the exact solution and Ψ' is the computed solution. In the following examples we will use the following measures to estimate the errors:

$$\begin{aligned} \varepsilon_{\text{MAX}} &= \max \|\Psi'_i - \Psi_i\| \\ \varepsilon_{\text{MSQ}} &= \sqrt{\frac{\sum_{i=1}^N (\Psi'_i - \Psi_i)^2}{n}} \\ \varepsilon_{\mathcal{L}^2} &= \sqrt{\frac{\sum_{i=1}^N (\Psi'_i - \Psi_i)^2}{\sum_{i=1}^N \Psi_i^2}}. \end{aligned}$$

EXAMPLE 1. We solve the Laplace equation in $[0, 1] \times [0, 1] \times [0, 1]$ with the boundary conditions corresponding to the harmonic solution (Table 1)

$$\Psi(x, y, z) = \frac{1}{\rho(x, y, z)},$$

where

$$\rho(x, y, z) = \sqrt{(x - x_0)^2 + (y - y_0)^2 + (z - z_0)^2}, \quad x_0 = y_0 = z_0 = -0.5.$$

One can observe that ε_{MAX} decreases a little bit less than what was predicted in the previous section according to the dominant error. After one subtraction step when the functions

TABLE 1
MAX, MSQ, and \mathcal{L}^2 Errors after One (Function Values on the Frame) and Two
(also Second Derivatives on the Frame) Subtraction Steps

| $N_x \times N_y \times N_z$ | One subtr. step | | | Two subtr. steps | | |
|-----------------------------|----------------------------|----------------------------|-------------------------------|----------------------------|----------------------------|-------------------------------|
| | ε_{MAX} | ε_{MSQ} | $\varepsilon_{\mathcal{L}^2}$ | ε_{MAX} | ε_{MSQ} | $\varepsilon_{\mathcal{L}^2}$ |
| $8 \times 8 \times 8$ | 1.3e-5 | 1.8e-6 | 3.0e-6 | 9.8e-7 | 8.1e-8 | 1.4e-7 |
| $16 \times 16 \times 16$ | 3.5e-6 | 2.3e-7 | 4.0e-7 | 8.1e-8 | 2.8e-9 | 4.7e-9 |
| $32 \times 32 \times 32$ | 9.3e-7 | 3.1e-8 | 5.2e-8 | 5.9e-9 | 8.8e-11 | 1.5e-10 |
| $64 \times 64 \times 64$ | 2.4e-7 | 3.9e-9 | 6.7e-9 | 4.0e-10 | 3.0e-12 | 5.0e-12 |

before the application of the Fourier transform are periodic, together with their derivatives, ε_{MAX} decreases a little bit less than four times as the number of points is doubled and the $\varepsilon_{\mathcal{L}^2}$ eight times. For two subtraction steps, when the functions after the subtraction procedure are periodic, together with their derivatives up to the third order, we obtain a decrease of about 16 and 32 times, respectively.

In the following examples we do not specify boundary conditions and only notice the corresponding exact solution. Examples 2–5 illustrate the same rate of convergence for various Dirichlet problems.

EXAMPLE 2. In $[0, \pi] \times [0, \pi] \times [0, \pi]$ the Dirichlet boundary problem is solved for the Laplace equation such that the exact solution is (Table 2)

$$\Psi(x, y, z) = \cos 2x \frac{\sinh \sqrt{3}(\pi - y)}{\sinh \sqrt{3}\pi} \frac{\sinh z}{\sinh \pi}.$$

EXAMPLE 3. The exact solution is (Table 3)

$$\Psi(x, y, z) = \cos 2x \cos y \frac{\sinh \sqrt{5}(\pi - z)}{\sinh \sqrt{5}\pi}, \quad (x, y, z) \in [0, \pi] \times [0, \pi] \times [0, \pi].$$

EXAMPLE 4. The same as Example 1, only $(x_0, y_0, z_0) = (-0.1, -0.3, -0.2)$ (Table 4).

EXAMPLE 5. The exact solution is (Table 5)

$$\Psi(x, y, z) = \sin 2x \frac{\sinh y}{\sinh \pi} \frac{\sinh z}{\sinh \pi}, \quad (x, y, z) \in [0, \pi] \times [0, \pi] \times [0, \pi].$$

TABLE 2
MAX, MSQ, and \mathcal{L}^2 Errors after One and Two Subtraction Steps

| $N_x \times N_y \times N_z$ | One subtr. step | | | Two subtr. steps | | |
|-----------------------------|----------------------------|----------------------------|-------------------------------|----------------------------|----------------------------|-------------------------------|
| | ε_{MAX} | ε_{MSQ} | $\varepsilon_{\mathcal{L}^2}$ | ε_{MAX} | ε_{MSQ} | $\varepsilon_{\mathcal{L}^2}$ |
| $8 \times 8 \times 8$ | 1.5e-4 | 1.5e-5 | 1.1e-4 | 4.2e-5 | 4.2e-6 | 3.3e-5 |
| $16 \times 16 \times 16$ | 4.4e-5 | 2.1e-6 | 2e-5 | 3.4e-6 | 1.3e-7 | 1.2e-6 |
| $32 \times 32 \times 32$ | 1.3e-5 | 2.9e-7 | 3e-6 | 2.4e-7 | 4.2e-9 | 4.4e-8 |
| $64 \times 64 \times 64$ | 3.8e-6 | 3.7e-8 | 4.2e-7 | 1.6e-8 | 1.3e-10 | 1.5e-9 |

TABLE 3
MAX, MSQ, and \mathcal{L}^2 Errors after One and Two Subtraction Steps

| $N_x \times N_y \times N_z$ | One subtr. step | | | Two subtr. steps | | |
|-----------------------------|----------------------------|----------------------------|-------------------------------|----------------------------|----------------------------|-------------------------------|
| | ε_{MAX} | ε_{MSQ} | $\varepsilon_{\mathcal{L}^2}$ | ε_{MAX} | ε_{MSQ} | $\varepsilon_{\mathcal{L}^2}$ |
| $8 \times 8 \times 8$ | 2.2e-4 | 3.2e-5 | 1.6e-4 | 8e-5 | 1e-5 | 5e-5 |
| $16 \times 16 \times 16$ | 2e-5 | 6.8e-7 | 4.5e-6 | 6.4e-6 | 3.6e-7 | 2.1e-6 |
| $32 \times 32 \times 32$ | 7e-5 | 5e-6 | 3e-5 | 4.3e-7 | 1.2e-8 | 8e-8 |
| $64 \times 64 \times 64$ | 5.4e-6 | 8.8e-8 | 6.2e-7 | 2.7e-8 | 3.9e-10 | 2.7e-9 |

2.7. Dirichlet Problems with Discontinuous Boundary Conditions or Boundary Conditions Which Do Not Satisfy the Laplace Equation

Everywhere above we assumed that the boundary function satisfies the Laplace equation on the edges and the corners. Let us assume now that for the edge $y = z = 0, 0 \leq x \leq 1$ the Laplace equation is not satisfied but

$$\frac{\partial^2 \Psi}{\partial x^2}(x, 0, \pi) + \frac{\partial^2 \Psi}{\partial y^2}(x, 0, \pi) + \frac{\partial^2 \Psi}{\partial z^2}(x, 0, \pi) = \varphi(x), \quad (2.15)$$

where $\varphi(x) \neq 0$. For instance, consider the case $\varphi(x) = ax + b$. The function

$$f(x, y, z) = \frac{ax + b}{2\pi} \left[2y(\pi - z) \ln \sqrt{y^2 + (\pi - z)^2} + \arctan \frac{\pi - z}{y} (y^2 - (\pi - z)^2) \right]$$

satisfies the Laplace equation everywhere except on the edge $y = 0, z = \pi$, where

$$\frac{\partial^2 f}{\partial x^2}(x, 0, \pi) + \frac{\partial^2 f}{\partial y^2}(x, 0, \pi) + \frac{\partial^2 f}{\partial z^2}(x, 0, \pi) = ax + b.$$

In fact,

$$\begin{aligned} f(x, 0, \pi) = 0 &\Rightarrow \frac{\partial^2 f}{\partial x^2}(x, 0, \pi) = 0, \\ f(x, y, \pi) = \frac{ax + b}{2\pi} \frac{\pi}{2} y^2 &\Rightarrow \frac{\partial^2 f}{\partial y^2}(x, 0, \pi) = \frac{ax + b}{2}, \\ f(x, 0, z) = \frac{ax + b}{2\pi} \frac{\pi}{2} (\pi - z)^2 &\Rightarrow \frac{\partial^2 f}{\partial z^2}(x, 0, \pi) = \frac{ax + b}{2}; \end{aligned}$$

TABLE 4
MAX, MSQ, and \mathcal{L}^2 Errors after One and Two Subtraction Steps

| $N_x \times N_y \times N_z$ | One subtr. step | | | Two subtr. steps | | |
|-----------------------------|----------------------------|----------------------------|-------------------------------|----------------------------|----------------------------|-------------------------------|
| | ε_{MAX} | ε_{MSQ} | $\varepsilon_{\mathcal{L}^2}$ | ε_{MAX} | ε_{MSQ} | $\varepsilon_{\mathcal{L}^2}$ |
| $8 \times 8 \times 8$ | 5.5e-5 | 3.8e-6 | 4.4e-6 | 3e-5 | 4e-6 | 4.7e-6 |
| $16 \times 16 \times 16$ | 1.7e-5 | 5.6e-7 | 6.5e-7 | 1.6e-6 | 5e-8 | 6e-8 |
| $32 \times 32 \times 32$ | 5.1e-6 | 7.7e-8 | 9e-8 | 1.3e-7 | 1.6e-9 | 1.9e-9 |
| $64 \times 64 \times 64$ | 1.5e-6 | 1e-8 | 1.2e-8 | 9.4e-9 | 5.2e-11 | 6e-11 |

TABLE 5
MAX, MSQ, and \mathcal{L}^2 Errors after One and Two Subtraction Steps

| $N_x \times N_y \times N_z$ | One subtr. step | | | Two subtr. steps | | |
|-----------------------------|----------------------------|----------------------------|-------------------------------|----------------------------|----------------------------|-------------------------------|
| | ε_{MAX} | ε_{MSQ} | $\varepsilon_{\mathcal{L}^2}$ | ε_{MAX} | ε_{MSQ} | $\varepsilon_{\mathcal{L}^2}$ |
| $8 \times 8 \times 8$ | 3.6e-5 | 3.9e-6 | 3.4e-5 | 5.8e-6 | 6.4e-7 | 5.5e-6 |
| $16 \times 16 \times 16$ | 1.1e-5 | 6.3e-7 | 6.3e-6 | 3.8e-7 | 2.8e-8 | 2.8e-7 |
| $32 \times 32 \times 32$ | 2.8e-6 | 8.6e-8 | 9.3e-7 | 1.7e-8 | 6.7e-10 | 7.3e-9 |
| $64 \times 64 \times 64$ | 7e-7 | 1.1e-8 | 1.3e-7 | 1e-9 | 1.6e-11 | 1.8e-10 |

therefore $\nabla^2 f(x, 0, \pi) = ax + b$. After subtraction of this function we obtain regular boundary conditions, and the technique that was developed in Sections 2.1–2.3 is applicable.

For the 2D case the problem of corner singularities was considered in [5, 17]. However, it is to be emphasized that in 3D the problem is more complicated. First, we have a singularity not only on a single point but on the whole edge. Second, in 3D we cannot apply methods of complex analysis which appeared to be useful for removing 2D singularities.

At first we describe some cases when singularity can be removed by subtraction of a function which is known analytically. Then a numerical method for the subtraction of singularities of a general type will be presented.

Some Types of Constant Singularities

1. Singularity from the intersection of two planes with different constant values:

$$\begin{aligned} \Psi(x, y, 0) = 1, \quad 0 < x, y \leq \pi, \quad \Psi(x, 0, z) = 0, \quad 0 \leq x, z \leq \pi, \\ \Psi(0, y, z) = 0, \quad 0 \leq y, z \leq \pi. \end{aligned}$$

The subtraction function for singularity removal is

$$u(x, y, z) = \frac{2}{\pi} \arctan \frac{xy}{z\sqrt{x^2 + y^2 + z^2}}.$$

2. A box with “a black floor and white walls”:

$$\begin{aligned} \Psi(x, y, 0) = 1, \quad 0 < x, y \leq \pi, \quad \Psi(x, 0, z) = \Psi(x, \pi, z) = 0, \quad 0 \leq x, z \leq \pi, \\ \Psi(0, y, z) = \Psi(\pi, y, z) = 0, \quad 0 \leq y, z \leq \pi. \end{aligned}$$

The corner singularity function is

$$\Phi(x, y, z) = \frac{1}{\pi} \left[\arctan \frac{x}{z} + \arctan \frac{y}{z} - 2 \arctan \frac{yx}{z\sqrt{x^2 + y^2 + z^2}} \right], \quad (2.16)$$

which corresponds to the corner $(0, 0, 0)$. The complete subtraction function which removes the singularities is

$$S(x, y, z) = 1 - \Phi(x, y, z) - \Phi(\pi - x, y, z) - \Phi(x, \pi - y, z) - \Phi(\pi - x, \pi - y, z).$$

3. A box with “black floor and ceiling and white walls”:

$$\Psi(x, y, 0) = 1, \quad \Psi(x, y, \pi) = 1, \quad 0 < x, y \leq \pi,$$

$$\Psi(x, 0, z) = \Psi(x, \pi, z) = 0, \quad 0 \leq x, z \leq \pi, \quad \Psi(0, y, z) = \Psi(\pi, y, z) = 0, \quad 0 \leq y, z \leq \pi.$$

TABLE 6
Numerical Accuracy after One Subtraction Step when the Solution Is Equal to One on the Bottom and Vanishes on All the Neighboring Faces

| $N_x \times N_y \times N_z$ | ε_{MAX} | ε_{MSQ} | $\varepsilon_{\mathcal{L}^2}$ |
|-----------------------------|----------------------------|----------------------------|-------------------------------|
| 16 × 16 × 16 | 2.0e-7 | 4.0e-8 | 2.0e-8 |
| 32 × 32 × 32 | 4.7e-8 | 3.5e-10 | 1.8e-9 |
| 64 × 64 × 64 | 1.2e-8 | 3.0e-11 | 1.7e-10 |

The harmonic function with the same singularity is $S(x, y, z) + S(x, y, \pi - z)$, where S stands for the function defined by (2.16).

EXAMPLE 6. Consider the second problem, i.e. the problem of a cube with a “black floor and white walls” (Table 6).

The General Case

The above results demonstrate that in the case when “a jump between the faces” is constant we usually can construct the subtraction function analytically. This leads to a smooth problem. Suppose now that $\Psi(x, 0+, 0) - \Psi(x, 0, 0+) = g(x)$.

The problem is how to build a function which has the same jump at the edge $z = y = 0$ and has no jumps on the other edges. This is equivalent to introducing a double layer at the face $y = 0$ with a fixed density $2g(x)$ at $z = 0$ and zero density at $z = 1$; for example, a subtraction function is introduced as

$$\varphi(x, y, z) = \frac{1}{2\pi} \int_0^1 \int_0^1 \frac{g(t)y \Phi(s) dt ds}{[(x-t)^2 + y^2 + (z-s)^2]^{3/2}},$$

where $\Phi(s)$ is a smooth function such that $\Phi(0) = 1$, $\Phi(1) = 0$. Obviously, $\Phi(s)$ is equal to zero at $y = 0$. We assume $g(0) = g(1) = 0$ to avoid a jump at the edges $(0, 0, z)$ and $(1, 0, z)$. This situation can be achieved by subtracting the corner singularities as shown in Fig. 5. Figure 6 illustrates the values on the faces $z = 0$ and $z = 1$ for the particular case $\Phi(s) = (1-s)^2$, $g(x) = \sin(\pi x)$. The function Φ has a jump at $z = 0$ and is smooth at $z = 1$.

3. POISSON EQUATION IN CUBE

The following problem involves the Poisson equation with boundary conditions on a rectangular box $B = (0, \pi) \times (0, \pi) \times (0, \pi)$:

$$\begin{aligned} \Psi_{xx} + \Psi_{yy} + \Psi_{zz} &= -F(x, y, z), & \text{Poisson equation,} \\ \Psi(0, y, z) = \Psi(\pi, y, z) &= 0 \quad \Psi(x, 0, z) = \Psi(x, \pi, z) = 0, & \text{boundary conditions,} \\ \Psi(x, y, 0) &= \Psi(x, y, \pi) = 0. \end{aligned} \tag{3.1}$$

To solve (3.1) we expand Ψ and F in triple sine series,

$$\begin{aligned} \Psi(x, y, z) &= \sum_{k,m,n=1}^{\infty} d_{kmn} \sin(kx) \sin(my) \sin(nz) \\ F(x, y, z) &= \sum_{k,m,n=1}^{\infty} D_{kmn} \sin(kx) \sin(my) \sin(nz), \end{aligned}$$

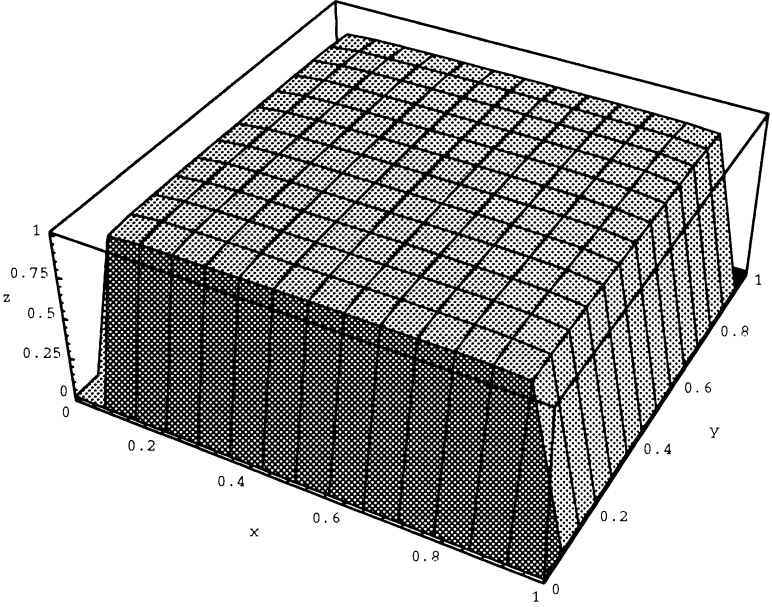


FIG. 5. Plot of the subtraction function $S(x, y, z)$ at $z=0.005$.

and substitute it into the Poisson equation (3.1) and, assuming that Ψ is twice continuously differentiable, we see that

$$d_{kmn} = \frac{D_{kmn}}{k^2 + m^2 + n^2}.$$

Thus,

$$\Psi(x, y, z) = \sum_{k,m,n=1}^{\infty} \frac{D_{kmn}}{k^2 + m^2 + n^2} \sin(kx) \sin(my) \sin(nz). \quad (3.2)$$

This series and its first and second partial derivatives converge absolutely and uniformly, provided the series F does the same. This is the case if F is extended as an odd function, it is continuously differentiable, and if the squares of its second derivatives have finite integrals. In this case Ψ is the solution of (3.1). The complete details are given in Appendix 3.

We proceed with the numerical algorithm for the solution of the Poisson equation. The numerical technique that locates a particular solution of the Poisson equation (3.1) includes the three-dimensional Fourier transform of the right-hand side. It is efficient and accurate if the right-hand side is periodic in the cube. If not, a smoothing procedure that includes extension and folding is applied on the right-hand side. Finally, the solution of the Dirichlet problem for the Poisson equation incorporates the following *steps*:

1. $F(x, y, z)$ is continuously extended to the domain $[-2\varepsilon, \pi + 2\varepsilon] \times [-2\varepsilon, \pi + 2\varepsilon] \times [-2\varepsilon, \pi + 2\varepsilon]$; this step can be omitted if the right-hand side is defined in the extended domain.

2. A one-dimensional folding procedure in z is applied to the extended function $\bar{F}(x, y, z)$ for each $-2\varepsilon \leq x, y \leq \pi + 2\varepsilon$. It is described in Appendix 4. As a result a new function $\bar{F}_1(x, y, z)$ is obtained which coincides with the original function in the cube $[0, \pi] \times [0, \pi] \times [0, \pi]$ and $\bar{F}_{1_z}^{(2r)}(x, y, -\varepsilon) = \bar{F}_1^{(2r)}(x, y, \pi + \varepsilon) = 0$, $r = 0, 1, \dots, -2\varepsilon \leq$

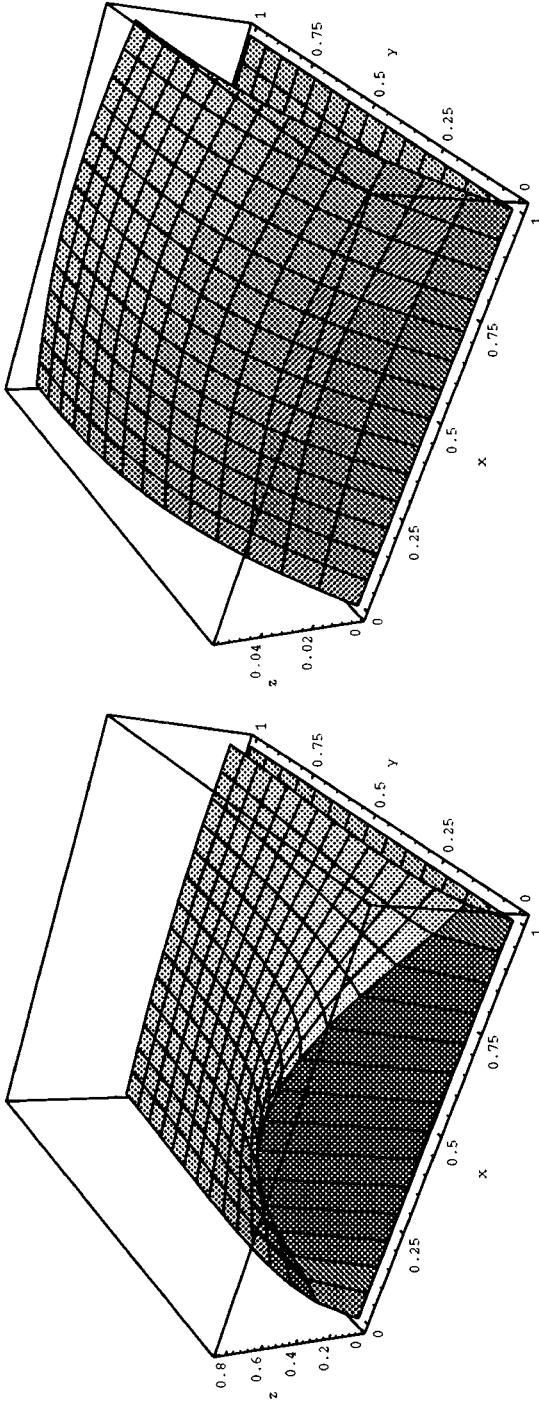


FIG. 6. The values of $\Phi(x, y, z)$ on the faces $z=0$ and $z=1$, respectively. On the face $y=0$ $\Phi(x, 0, z) \equiv 0$.

$x, y \leq \pi + 2\varepsilon$. The cost of this step is $O((N + N_\varepsilon)^2 \cdot N_\varepsilon)$, where N_ε is the number of discretization points on the extended segment. N_ε is small when it is compared with N .

3. The same folding procedure in y , for each $-2\varepsilon \leq x \leq \pi + 2\varepsilon$, $-\varepsilon \leq z \leq \pi + \varepsilon$, leads to the function \bar{F}_2 which is periodic, together with its even derivatives in y : $\bar{F}_{2y}^{(2r)}(x, -\varepsilon, z) = \bar{F}_1^{(2r)}(x, \pi + \varepsilon, z) = 0, r = 0, 1, \dots, -2\varepsilon \leq x \leq \pi + 2\varepsilon, -\varepsilon \leq z \leq \pi + \varepsilon$. The cost is $O((N + N_\varepsilon) \cdot N \cdot N_\varepsilon)$.

4. Folding procedure in x for each $-\varepsilon \leq y, z \leq \pi + \varepsilon$ generates a function \bar{F}_3 periodic in “the extended cube”

$$[-\varepsilon, \pi + \varepsilon] \times [-\varepsilon, \pi + \varepsilon] \times [-\varepsilon, \pi + \varepsilon],$$

together with its even derivatives in x, y , and z . The cost of this step is $O(N^2 \cdot N_\varepsilon)$.

5. The Poisson equation (3.1) is solved in the extended domain; the solution is effective and accurate due to periodicity of the extended right-hand side \bar{F}_3 which coincides with the original right-hand side in the original domain. The restriction of the obtained solution to the cube $[0, \pi] \times [0, \pi] \times [0, \pi]$ is a particular solution of the Poisson equation which satisfies some boundary conditions. The procedure requires $O(N^3 \log_2 N)$ operations which is crucial for the algorithm.

6. An additional Laplace equation is solved with boundary conditions which are equal to the difference between the original conditions and those of the particular solution of the Poisson equation that was obtained in the previous step. When the solution of the Laplace equation is added to the solution of the Poisson equation we obtain a solution of the problem. As shown in Section 2.4 this part of the algorithm can be implemented with $O(N^3 \log_2 N)$ operations. Consequently, the solution of the Poisson equation requires $O(N^3 \log_2 N)$ operations.

EXAMPLE 7. The right-hand side is one of the following functions:

$$F(x, y, z) = \sin(4x) \sin(4y) \sin(4z),$$

| | | |
|----------|----------|------------|
| $\sin x$ | $\sin y$ | $\sin z$, |
| $\cos x$ | $\cos y$ | $\cos z$ |

The results are obtained by successive application of the program that computes a particular solution of the nonhomogeneous equation and the program for the Laplace equation (Table 7).

EXAMPLE 8. The right-hand side is (Table 8)

$$f(x, y, z) = \exp\{-\alpha((x - 0.5)^2 + (y - 0.5)^2 + (z - 0.5)^2)\}.$$

The results are obtained by successive application of the program that computes a particular solution of the nonhomogeneous equation and the program for the Laplace equation.

For $\alpha = 3$ Table 9 shows the dependence of the accuracy on the length of the extension interval. Everywhere below $(32 + 1)^3$ points are taken in the box $[0, 1]^3$, while the number of folding points (equal in each direction) varies.

TABLE 7

Maximal, MSQ, and \mathcal{L}^2 Errors for the Numerical Solution of the Poisson Equation (3.1)

| $F(x, y, z)$ | $N_x \times N_y \times N_z$ | Fold. points | ε_{MAX} | ε_{MSQ} | $\varepsilon_{\mathcal{L}^2}$ |
|------------------------------|-----------------------------|--------------|----------------------------|----------------------------|-------------------------------|
| $\sin(4x) \sin(4y) \sin(4z)$ | $8 \times 8 \times 8$ | 4 | 2.6e-6 | 4.3e-7 | 6.9e-4 |
| | $16 \times 16 \times 16$ | 8 | 7.9e-9 | 1.9e-9 | 2.7e-6 |
| | $32 \times 32 \times 32$ | 16 | 1.7e-12 | 1.3e-13 | 1.8e-10 |
| $\sin x \sin y \sin z$ | $8 \times 8 \times 8$ | 4 | 1.9e-6 | 7.5e-7 | 7.5e-5 |
| | $16 \times 16 \times 16$ | 8 | 1.9e-9 | 6.9e-10 | 6.4e-8 |
| | $32 \times 32 \times 32$ | 16 | 4.7e-11 | 4.4e-12 | 3.9e-10 |
| $\cos x \cos y \cos z$ | $8 \times 8 \times 8$ | 4 | 1.2e-6 | 2.0e-7 | 1.5e-5 |
| | $16 \times 16 \times 16$ | 8 | 1.1e-9 | 2.1e-10 | 1.6e-8 |
| | $32 \times 32 \times 32$ | 16 | 8.2e-11 | 1.4e-12 | 1.1e-10 |

4. SUMMARY AND DISCUSSION

We developed a spectral algorithm which has the following properties:

1. The algorithm provides fast convergence (in fact, any prescribed rate of convergence) which leads to high accuracy for comparatively small number of grid points in each direction (the error $10^{-7} - 10^{-9}$ is achieved for 32 grid points in each direction when two subtraction steps are applied).

2. The algorithm requires the same order of operations as the usual Fourier method requires which is $O(N^3 \log N)$. Here N is the number of grid points in each direction. The cost of each subtraction step is $O(N^3)$, which is asymptotically smaller than the cost of the application of the Fourier transform.

For example, we consider the Dirichlet problem for the Laplace equation with the boundary conditions corresponding to the exact solution

$$\Psi(x, y, z) = \frac{1}{\sqrt{(x+0.1)^2 + (y+0.3)^2 + (z+0.2)^2}}.$$

Table 10 shows the numerical results of the straightforward application of the Fourier

TABLE 8

The Dependence of the Numerical Accuracy on the Number of Grid Points and the Steepness of the Gaussian

| α | $N_x \times N_y \times N_z$ | Fold. points | ε_{MAX} | ε_{MSQ} | $\varepsilon_{\mathcal{L}^2}$ |
|----------|-----------------------------|--------------|----------------------------|----------------------------|-------------------------------|
| 0.5 | $8 \times 8 \times 8$ | 4 | 4.2e-6 | 1.7e-6 | 2.0e-6 |
| | $16 \times 16 \times 16$ | 8 | 3.6e-7 | 1.8e-8 | 2.0e-8 |
| | $32 \times 32 \times 32$ | 16 | 8.9e-8 | 1.9e-9 | 2.1e-9 |
| 3 | $8 \times 8 \times 8$ | 4 | 3.4e-6 | 1.5e-6 | 3.1e-6 |
| | $16 \times 16 \times 16$ | 8 | 1.0e-8 | 1.7e-9 | 3.4e-9 |
| | $32 \times 32 \times 32$ | 16 | 2.8e-9 | 6.0e-11 | 1.2e-10 |
| 15 | $8 \times 8 \times 8$ | 4 | 2.8e-6 | 4.2e-7 | 2.7e-6 |
| | $16 \times 16 \times 16$ | 8 | 1.6e-12 | 4.9e-13 | 2.9e-12 |
| | $32 \times 32 \times 32$ | 16 | 6.2e-15 | 5.1e-16 | 2.3e-15 |

TABLE 9

Dependence of the Numerical Accuracy on the Number of Folding Points

| Fold. points | ε_{MAX} | ε_{MSQ} | $\varepsilon_{\mathcal{L}^2}$ |
|--------------|----------------------------|----------------------------|-------------------------------|
| 4 | 2.0e-7 | 5.4e-8 | 1.0e-7 |
| 8 | 1.1e-8 | 3.3e-10 | 6.3e-10 |
| 11 | 7.3e-9 | 1.6e-10 | 3.1e-10 |
| 14 | 4.3e-9 | 9.3e-11 | 1.8e-10 |
| 16 | 2.8e-9 | 6.0e-11 | 1.2e-10 |
| 20 | 1.1e-9 | 2.2e-11 | 4.3e-11 |
| 24 | 3.5e-10 | 9.7e-12 | 1.8e-11 |

transform without subtraction. They are compared to the results of the algorithm developed in this paper using the two subtraction steps. Due the Gibbs phenomenon that exists since the function is not periodic we can see that the error ε_{MAX} is constant since it is stipulated by the “jump” of the function at the end. The average errors ε_{MSQ} and $\varepsilon_{\mathcal{L}^2}$ decay as $1/N$, where N is the number of grid points in each direction.

The present algorithm, that computes the solution of the Poisson equation fast in a regular 3D domain, is a part of a more general algorithm. Suppose that we solve a Dirichlet problem for the Poisson equation

$$\Delta u(x, y, z) = f(x, y, z), \quad (x, y, z) \in \Omega, \quad U(x, y, z) = \phi(x, y, z), \quad (x, y, z) \in \partial\Omega,$$

in a 3D domain Ω with complex geometry. The domain Ω is decomposed into some subdomains that have regular geometry and only few subdomains have complex geometry (which are located near the boundary). In each subdomain a different resolution is chosen that depends on the smoothness of the right-hand side f . This makes the algorithm adaptive. The Poisson equation in domains of complex geometry can be solved similar to [20], where the 2D case was considered. If the equation

$$\Delta u(x, y, z) = f(x, y, z)$$

was solved in each subdomain, the collection of these solutions may have discontinuities at the domain interfaces. The matching procedure for domains with different resolutions was developed in [7].

TABLE 10

Comparison between the Numerical Results That Were Derived from the Application of the Fourier Method (without Subtraction Steps) and the Present Algorithm with Two Subtraction Steps

| $N_x \times N_y \times N_z$ | Fourier method without subtraction | | | Two subtraction steps | | |
|-----------------------------|------------------------------------|----------------------------|-------------------------------|----------------------------|----------------------------|-------------------------------|
| | ε_{MAX} | ε_{MSQ} | $\varepsilon_{\mathcal{L}^2}$ | ε_{MAX} | ε_{MSQ} | $\varepsilon_{\mathcal{L}^2}$ |
| $8 \times 8 \times 8$ | 2.8 | 3.6e-1 | 5.3e-1 | 3e-5 | 4e-6 | 4.7e-6 |
| $16 \times 16 \times 16$ | 2.8 | 2.0e-1 | 2.9e-1 | 1.6e-6 | 5e-8 | 6e-8 |
| $32 \times 32 \times 32$ | 2.8 | 1.0e-1 | 1.5e-1 | 1.3e-7 | 1.6e-9 | 1.9e-9 |
| $64 \times 64 \times 64$ | 2.8 | 5.2e-2 | 7.6e-2 | 9.4e-9 | 5.2e-11 | 6e-11 |

The results of this paper can be extended in two directions:

1. Elliptic equations of a more general type can be considered, for example, the Helmholtz equation. This is critical for computational fluid dynamics problems. Discretization of the Navier–Stokes equation leads to a Helmholtz equation at each time step.
2. The Neumann/mixed problem can be solved for the Poisson equation.

The paper [6] includes fast spectral solvers both for the Dirichlet problem for the 3D Helmholtz equation and for the Neumann/mixed boundary problem for the Poisson equation.

APPENDIX 1: SOLUTION OF THE LAPLACE EQUATION BY FOURIER SERIES

We discuss now the validity of (2.4) as a solution to (2.1). Similar arguments apply to the other series that occur in solving Dirichlet’s problem in the cube C .

Suppose that $|D_{mn}| \leq A$, a constant, for all m and n . This is certainly true if

$$\int_0^\pi \int_0^\pi |f(x, y)| dx dy$$

is finite. If $0 \leq z \leq \pi - \delta$ for $\delta > 0$, then

$$0 \leq A \frac{\sinh \delta_{mn} z}{\sinh \delta_{mn} \pi} = A \frac{e^{\delta_{mn} z}}{e^{-\delta_{mn} \pi}} \frac{1 - e^{-2\delta_{mn} z}}{e^{2\delta_{mn} \pi} - 1} \leq A e^{-\delta_{mn} \delta} \frac{1}{e^{2\sqrt{2}\pi} - 1}$$

and $\sum_{m,n=1}^\infty A e^{-\delta_{mn} \delta} [e^{2\sqrt{2}\pi} - 1]^{-1}$ converges by the comparison test. It follows that

$$\sum_{m,n=1}^\infty D_{mn} \sin mx \sin ny (\sinh \delta_{mn} z / \sinh \delta_{mn} \pi) \quad (4.3)$$

converges uniformly to Ψ for $0 \leq z \leq \pi - \delta$. Similar arguments show that (4.3) may be differentiated term by term any number of times, provided that $0 \leq z \leq \pi - \delta$. Hence, letting δ approach zero, we find that Ψ is harmonic in C .

If f_1 is C^2 when extended as an odd periodic function, then Ψ satisfies the boundary conditions of Dirichlet’s problem.

Finally, we note that the uniqueness of Ψ follows by the maximum–minimum principle for harmonic functions.

APPENDIX 2: ONE STEP SUBTRACTION PROCEDURE

If in (2.6) all $d_n \neq 0$, the function values at the edges and the second derivatives can be subtracted simultaneously. We observe that in (2.6)–(2.10) $\lambda_{1n}, \lambda_{2n}$ are not uniquely determined. They can be chosen such that the second derivatives have the appropriate values.

The functions $\Psi(x, 0, \pi)$, $(\partial^2 \Psi / \partial y^2)(x, 0, \pi)$ can be expressed as

$$\Psi(x, 0, \pi) \sim \sum_{n=1}^\infty d_n \sin nx, \quad \frac{\partial^2 \Psi}{\partial y^2}(x, 0, \pi) \sim \sum_{n=1}^\infty b_n \sin nx, \quad (4.4)$$

where

$$d_n = \frac{2}{\pi} \int_0^\pi \Psi(x, 0, \pi) \sin nx \, dx, \quad b_n = \frac{2}{\pi} \int_0^\pi \frac{\partial^2 \Psi}{\partial y^2}(x, 0, \pi) \sin nx \, dx. \quad (4.5)$$

Let us set

$$\begin{aligned} \lambda_{1n}^2 &= b_n/d_n, \\ \lambda_{2n} &= \sqrt{n^2 - \lambda_{1n}^2}, \quad \text{if } n > \lambda_{1n} \text{ in (2.6),} \\ \lambda_{2n} &= \sqrt{\lambda_{1n}^2 - n^2}, \quad \text{if } n < \lambda_{1n} \text{ in (2.7),} \end{aligned} \quad (4.6)$$

if $b_n/d_n > 0$,

$$\begin{aligned} \lambda_{1n}^2 &= -b_n/d_n, \quad \lambda_{2n} = \sqrt{\lambda_{1n}^2 + n^2}, \\ u_1^*(x, y, z) &= \sum_{n=1}^{\infty} d_n \sin nx \frac{\sin \lambda_{1n}(\pi - y)}{\sin \lambda_{1n}\pi} \frac{\sinh \lambda_{2n}z}{\sinh \lambda_{2n}\pi}, \end{aligned} \quad (4.7)$$

if $b_n/d_n < 0$.

Then, after subtraction of u_1 the function vanishes with its second partial derivatives in y and z on the edge (the boundary conditions satisfy the Laplace equation on the edges).

This procedure is not applicable if at least one $d_n = 0$.

Similar procedure can be applied to the corners. Consider the corner $(0, 0, 0)$. If $\Psi(0, 0, 0) = A \neq 0$, then by the appropriate choice of λ_1, λ_2 in (2.14) we can in fact achieve the annihilation of the three second derivatives with repeated indices. For example, if $B_y = (\partial^2 \Psi / \partial y^2)(0, 0, 0) > 0$, $B_z = (\partial^2 \Psi / \partial z^2)(0, 0, 0) < 0$, $-B_z > B_y$, then $\lambda_2 = \sqrt{B_y}$, $\lambda_3 = \sqrt{-B_z}$, $\lambda_1 = \sqrt{\lambda_3^2 - \lambda_2^2}$. If also $B_y < 0$, then we choose the ‘‘corner function’’ as

$$C_{(0,0,0)}(x, y, z) = \Psi(0, 0, 0) \left[\frac{\sinh \lambda_1(\pi - x)}{\sinh \lambda_1\pi} \frac{\sin \lambda_2(\pi - y)}{\sin \lambda_2\pi} \frac{\sin \lambda_3(\pi - z)}{\sin \lambda_3\pi} \right] \quad (4.8)$$

with

$$\lambda_2^2 = -\frac{\partial^2 \Psi}{\partial y^2}(0, 0, 0) = -B_y, \quad \lambda_3^2 = -\frac{\partial^2 \Psi}{\partial z^2}(0, 0, 0) = -B_z, \quad \lambda_1 = \sqrt{\lambda_3^2 + \lambda_2^2}.$$

In case $B_y > 0$, $B_z < 0$, $-B_z, B_y$ the function

$$C_{(0,0,0)}(x, y, z) = A \left[\frac{\sin \lambda_1(\pi - x)}{\sin \lambda_1\pi} \frac{\sinh \lambda_2(\pi - y)}{\sinh \lambda_2\pi} \frac{\sin \lambda_3(\pi - z)}{\sin \lambda_3\pi} \right]$$

is subtracted, wherein $\lambda_2 = \sqrt{B_y}$, $\lambda_3 = \sqrt{-B_z}$, $\lambda_1 = \sqrt{\lambda_2^2 - \lambda_3^2}$, etc.

APPENDIX 3: GREEN FUNCTION FOR THE POISSON EQUATION

By the Parseval equation we can write the solution (3.2) as

$$\Psi(x, y, z) = \int_0^\pi \int_0^\pi \int_0^\pi G(x, y, z; \xi, \eta, \zeta) F(\xi, \eta, \zeta) d\xi d\eta d\zeta, \quad (4.9)$$

provided G is a function such that

$$G(x, y, z; \xi, \eta, \zeta) \sim \frac{8}{\pi^3} \sum \sum \sum \frac{\sin kx \sin my \sin nz \sin k\xi \sin m\eta \sin n\zeta}{k^2 + m^2 + n^2}. \quad (4.10)$$

To find this function we let

$$r = \sqrt{(\xi - x)^2 + (\eta - y)^2 + (\zeta - z)^2}$$

and choose a constant a depending upon the fixed point (x, y, z) in such a way that the sphere $r \leq a$ inside our cube. We define the function

$$\psi(r) = \begin{cases} \frac{1}{2r} \left[5 \left(1 - \frac{r}{a} \right)^4 - 3 \left(1 - \frac{r}{a} \right)^5 \right], & r < a, \\ 0, & r \geq a. \end{cases}$$

Then, $\psi(r) - 1/r$ has a continuous second partial derivatives, bounded third derivatives, and square integrable fourth derivatives.

We expand $\psi(r)$ in a triple sine series. Making the change of variable

$$\xi' = \xi - x, \quad \eta' = \eta - y, \quad \zeta' = \zeta - z,$$

we let

$$\begin{aligned} \frac{\pi^3}{8} A_{kmn} &= \int_0^\pi \int_0^\pi \int_0^\pi \psi(\sqrt{(\xi - x)^2 + (\eta - y)^2 + (\zeta - z)^2}) \sin k\xi \sin m\eta \sin n\zeta \, d\xi \, d\eta \, d\zeta \\ &= \iiint_{\xi'^2 + \eta'^2 + \zeta'^2 < a^2} \psi(\sqrt{\xi'^2 + \eta'^2 + \zeta'^2}) \\ &\quad \times \sin k(\xi' + x) \sin m(\eta' + y) \sin n(\zeta' + z) \, d\xi' \, d\eta' \, d\zeta' \\ &= \iiint \psi[\sin k\xi' \cos kx + \cos k\xi' \sin kx][\sin m\eta' \cos my + \cos m\eta' \sin my] \\ &\quad \times [\sin n\zeta' \cos nz + \cos n\zeta' \sin nz] \, d\xi' \, d\eta' \, d\zeta' \\ &= \sin kx \sin my \sin nz \iiint \psi \cos k\xi' \cos m\eta' \cos n\zeta' \, d\xi' \, d\eta' \, d\zeta'. \end{aligned}$$

(Since ψ is even in ξ' , η' , and ζ' , integrals of $\psi \sin \xi'$, $\psi \sin \eta'$, and $\psi \sin \zeta'$ are zero.)

Now

$$\begin{aligned} \cos k\xi' \cos m\eta' \cos n\zeta' &= \frac{1}{4} [\cos(l\xi' + m\eta' + n\zeta') + \cos(l\xi' + m\eta' - n\zeta') \\ &\quad + \cos(l\xi' - m\eta' + n\zeta') + \cos(l\xi' - m\eta' - n\zeta')]. \end{aligned}$$

Since ψ is even in ξ' , η' , and ζ' , we find that the integrals of ψ times each of these cosines gives the same result. Then,

$$\frac{\pi^3}{8} A_{kmn} = \iiint_{\xi'^2 + \eta'^2 + \zeta'^2 < a^2} \psi(\sqrt{\xi'^2 + \eta'^2 + \zeta'^2}) \cos(k\xi' + m\eta' + n\zeta') \, d\xi' \, d\eta' \, d\zeta'.$$

We now use the spherical coordinates (r, θ, ϕ) with origin at (x, y, z) and the polar axis in the direction of the vector with components (k, m, n) . Then,

$$\begin{aligned}\sqrt{\xi'^2 + \eta'^2 + \zeta'^2} &= r, \\ k\xi' + m\eta' + n\zeta' &= r\sqrt{k^2 + m^2 + n^2} \cos \theta,\end{aligned}$$

and, hence,

$$\frac{\pi^3}{8} A_{kmn} = \int_0^a \int_0^\pi \int_0^{2\pi} \psi(r) \cos(r\sqrt{k^2 + m^2 + n^2} \cos \theta) r^2 \sin \theta \, dr \, d\theta \, d\phi.$$

We investigate first with respect to ϕ and then with respect to θ :

$$\begin{aligned}\frac{\pi^3}{8} A_{kmn} &= 2\pi \int_0^a \psi(r) \left[\frac{-\sin(r\sqrt{k^2 + m^2 + n^2} \cos \theta)}{r\sqrt{k^2 + m^2 + n^2}} \right]_0^\pi r^2 \, dr \\ &= \frac{4\pi}{\sqrt{k^2 + m^2 + n^2}} \int_0^a \psi(r) r \sin(r\sqrt{k^2 + m^2 + n^2}) \, dr.\end{aligned}$$

Using the definition of ψ , we find

$$\begin{aligned}A_{kmn} &= \frac{32}{\pi^2(k^2 + m^2 + n^2)} \left[1 - \frac{60(2 + \cos a\sqrt{k^2 + m^2 + n^2})}{a^4(k^2 + m^2 + n^2)^2} \right. \\ &\quad \left. + \frac{180 \sin a\sqrt{k^2 + m^2 + n^2}}{a^5(k^2 + m^2 + n^2)^{5/2}} \right] \sin kx \sin my \sin nz.\end{aligned}$$

Thus,

$$\begin{aligned}\frac{1}{4\pi} \psi(r) &\sim \frac{8}{\pi^3} \sum \sum \sum \left[\frac{1}{k^2 + m^2 + n^2} - \frac{60(2 + \cos a\sqrt{k^2 + m^2 + n^2})}{a^4(k^2 + m^2 + n^2)^3} \right. \\ &\quad \left. + \frac{180 \sin a\sqrt{k^2 + m^2 + n^2}}{a^5(k^2 + m^2 + n^2)^{7/2}} \right] \sin kx \sin my \sin nz \sin k\xi \sin m\eta \sin n\zeta.\end{aligned}$$

Comparing with (4.10), we see that

$$\begin{aligned}G(x, y, z; \xi, \eta, \zeta) &= \frac{1}{4\pi} \psi(r) \frac{480}{\pi^3} \sum_1^\infty \sum_1^\infty \sum_1^\infty \left[\frac{2 + \cos a\sqrt{k^2 + m^2 + n^2}}{a^4(k^2 + m^2 + n^2)^3} \right. \\ &\quad \left. - \frac{3 \sin a\sqrt{k^2 + m^2 + n^2}}{a^5(k^2 + m^2 + n^2)^{7/2}} \right] \sin kx \sin my \sin nz \sin k\xi \sin m\eta \sin n\zeta.\end{aligned}\tag{4.11}$$

The series on the right and its first and second partial derivatives converge uniformly. This means that $G - 1/(4\pi r)$ is twice continuously differentiable and that G vanishes on the faces of the cube. It can be verified by direct differentiation that

$$\nabla^2 \left(\frac{1}{r} \right) = 0 \quad \text{for } r \neq 0$$

and that

$$\nabla^2[\psi(r)] = \frac{1}{r} \frac{d^2}{dr^2}(r\psi) \quad \text{for } r \neq 0.$$

From this it follows that the Laplacian of the series is the series of $-(1/4\pi)\nabla^2\psi$. Hence, $\nabla^2 G = 0$.

The function G is called the Green's function. For a general domain D the Green's function G is characterized by the properties

1. $\nabla^2 G = 0$ in D ,
2. $G = 0$ on the boundary,
- 3.

$$G(x, y, z; \xi, \eta, \zeta) = \frac{1}{4\pi \sqrt{(x - \xi)^2 + (y - \eta)^2 + (z - \zeta)^2}} - \gamma(x, y, z; \xi, \eta, \zeta),$$

where γ is a regular solution of Laplace's equation. Such a Green's function exists for any sufficiently regular bounded domain. However, it can usually not be found explicitly. As in two dimensions, G is symmetric:

$$G(x, y, z; \xi, \eta, \zeta) = G(\xi, \eta, \zeta; x, y, z)$$

Physically, G is the potential at (x, y, z) due to a charge at (ξ, η, ζ) inside a cubical box whose sides are kept at zero potential.

The function γ in condition (3) is the solution of the boundary value problem

$$\begin{aligned} \nabla^2 \gamma &= 0, & \text{in } D, \\ \gamma &= \frac{1}{4\pi \sqrt{(x - \xi)^2 + (y - \eta)^2 + (z - \zeta)^2}}, & \text{on the boundary.} \end{aligned}$$

It is infinitely differentiable in D . Hence, the same is true for G except at (x, y, z) .

By using the form (4.11) of the Green function we can show that the function (4.9) satisfies the Poisson equation (3.1) if F is continuous and continuously differentiable. Under these hypotheses we see from the Schwarz inequality and the Parseval equation that the series (3.2) converges uniformly, so that Ψ also satisfies the boundary conditions of the problem (3.1).

APPENDIX 4: FOLDING PROCEDURE

To implement the smoothing, we introduce the bell function $B(x)$, supported on the extended interval $a_1 < a < b < b_1$,

$$\begin{aligned} B^2(x) + B^2(2\bar{a} - x) &= 1, & x \in [a_1, a], \\ B(x) &= 1, & x \in [a, b], \\ B^2(x) + B^2(2\bar{b} - x) &= 1, & x \in [b, b_1], \\ B(x) &= 0, & x < a_1, x > b_1, \end{aligned} \tag{4.12}$$

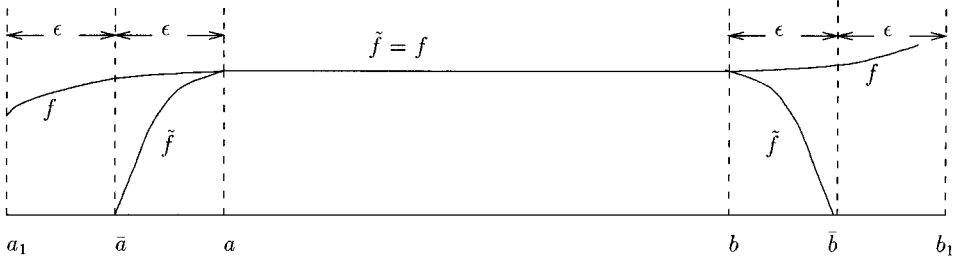


FIG. 7. The folding operation.

where $\bar{a} = (a + a_1)/2$, $\bar{b} = (b + b_1)/2$. This function is equal to $B = 1$ inside the subdomain and smoothly decays outwards over the distance $2\epsilon = b_1 - b = a - a_1$. Some particular forms of $B(x)$ were tested in [13, 14].

The smoothing of the function f , denoted by \tilde{f} , appears as a “folding” across the lines \bar{a} and \bar{b} (see Fig. 7):

$$\tilde{f} \equiv B \cdot f = \mathcal{F}_{\bar{a}} \mathcal{F}_{\bar{b}} f(x) = B(x) f(x) - B(2\bar{a} - x) f(2\bar{a} - x) - B(2\bar{b} - x) f(2\bar{b} - x) \quad (4.13)$$

(the “folded” function \tilde{f} is defined in $[\bar{a}, \bar{b}]$; the second term is “switched on” only in the interval $x \in [a_1, a]$ and the third term in the interval $x \in [b, b_1]$, respectively). The extra pieces of the function f , required for the smoothing operation, are provided by overlapping the neighboring subdomains over 4ϵ range. On the interval $x \in [a, b]$ we have $\tilde{f} = f$.

The smoothing procedure keeps the function \tilde{f} highly continuous at $x = a, b$. In addition, Eq. (4.13) yields that in the vicinity of the points $x = \bar{a}$, $x = \bar{b}$ the function $\tilde{f}(x)$ is odd and thus all even derivatives $\tilde{f}^{(2r)}(\bar{a}) = \tilde{f}^{(2r)}(\bar{b}) = 0$ for $r = 0, 1, \dots$. After an antisymmetric reflection across the point $x = \bar{b}$ (or $x = \bar{a}$) is performed, we obtain a smooth periodic function which can be represented by a rapidly converging sine series.

In the numerical implementation of the algorithm the bell was used,

$$B(x) = \begin{cases} 0, & x < a_1 \text{ or } x > b_1, \\ \sin(\theta(x)), & x \in [a_1, a], \\ 1, & x \in [a, b] \\ \cos(\theta(x)), & x \in [b, b_1] \end{cases} \quad (4.14)$$

with

$$\theta(x) = \frac{\pi}{4} \left(1 + \sin \left(\frac{\pi}{2} \sin \left(\sin \left(\frac{\pi x}{2\epsilon} \right) \right) \right) \right). \quad (4.15)$$

REFERENCES

1. G. Aharoni, A. Averbuch, R. Coifman, and M. Israeli, Local cosine transform—A method for the reduction of the blocking effect in JPEG, *J. Math. Imaging Vision* **3**, 7 (1993).
2. A. Averbuch, G. Beylkin, R. Coifman, and M. Israeli, Multiscale inversion of elliptic operators, in *The Samuel Neaman Workshop on Signal and Image Representation in Combined Space, Technion, Haifa, Israel, May 8–11, 1994*, edited by Y. Zeevi and R. Coifman (Academic Press, San Diego, 1998), p. 341.

3. A. Averbuch, G. Beylkin, R. Coifman, P. Fischer, and M. Israeli, Adaptive solution of multidimensional PDEs via tensor product wavelet decomposition, in preparation.
4. A. Averbuch, M. Israeli, and L. Vozovoi, A fast Poisson solver of arbitrary order accuracy in rectangular regions, *SIAM J. Sci. Comput.*, to appear.
5. A. Averbuch, M. Israeli, and L. Vozovoi, On fast direct elliptic solver by modified Fourier method, *Numer. Algorithms* **15**(3, 4), 287 (1997).
6. E. Braverman, M. Israeli, and A. Averbuch, A fast spectral solver for 3-D Helmholtz equation, in preparation.
7. E. Braverman, M. Israeli, and A. Averbuch, Parallel adaptive solution of a Poisson equation with multi-wavelets, in preparation.
8. C. Canuto, M. Y. Hussaini, A. Quarteroni, and T. A. Zang, *Spectral Methods in Fluid Dynamics* (Springer-Verlag, New York/Berlin, 1989).
9. T. Chan, R. Glowinsky, J. Peériaux, and O. Widlund (Eds.), *Domain Decomposition Methods* (SIAM, Philadelphia, 1989).
10. D. Gottlieb and S. A. Orszag, *Numerical Analysis of Spectral Methods: Theory and Applications* (SIAM, Philadelphia, 1977).
11. L. Greengard and J.-Y. Lee, A direct adaptive Poisson solver of arbitrary order accuracy, *J. Comput. Phys.* **125**, 415 (1996).
12. L. Greengard and V. Rokhlin, A fast algorithm for particle simulations, *J. Comput. Phys.* **73**, 325 (1978).
13. M. Israeli, L. Vozovoi, and A. Averbuch, Domain decomposition methods for solving parabolic PDEs on multiprocessors, *Appl. Numer. Math.* **12**, 193 (1993).
14. M. Israeli, L. Vozovoi, and A. Averbuch, Spectral multi-domain technique with local Fourier basis, *J. Sci. Comput.* **8**, 135 (1993).
15. S. McCormick, *Multigrid Methods* (SIAM, Philadelphia, 1987).
16. A. McKenney, L. Greengard, and A. Mayo, A fast Poisson solver for complex geometries, *J. Comput. Phys.* **118**, 348 (1995).
17. M. R. Schumack, W. W. Schultz, and J. P. Boyd, Spectral method solution of the Stokes equations on non-staggered grids, *J. Comput. Phys.* **94**, 30 (1991).
18. G. Skölermo, A Fourier method for numerical solution of Poisson's equation, *Math. Comput. (U.S.A.)* **29**, 697 (1975).
19. L. Vozovoi, M. Israeli, and A. Averbuch, Spectral multi-domain technique with local Fourier basis II: Decomposition into cells, *J. Sci. Comput.* **9**, 311 (1994).
20. L. Vozovoi, M. Israeli, and A. Averbuch, Multidomain local Fourier method for PDEs in complex geometries, *J. Comput. Applied Math.* **66**, 543 (1996).